Low-frequency current noise of the single-electron shuttle

2004 Europhys. Lett. 66 708

(http://iopscience.iop.org/0295-5075/66/5/708)

EUROPHYSICS LETTERS 1 June 2004

Europhys. Lett., **66** (5), pp. 708–714 (2004)
DOI: 10.1209/epl/i2004-10024-x

Low-frequency current noise of the single-electron shuttle

A. Isacsson[1,2] and T. Nord[1]

[1] *Department of Applied Physics, Chalmers University of Technology and Göteborg University - SE-412 96 Göteborg, Sweden*
[2] *Department of Physics, Yale University - P.O. Box 208120 New Haven, CT 06520-8120, USA*

(received 9 February 2004; accepted in final form 30 March 2004)

PACS. 73.23.Hk – Coulomb blockade; single-electron tunneling.
PACS. 72.70.+m – Noise processes and phenomena.
PACS. 85.85.+j – Micro- and nano-electromechanical systems (MEMS/NEMS) and devices.

Abstract. – Coupling between electronic and mechanical degrees of freedom in a single-electron shuttle system can cause a mechanical instability leading to shuttle transport of electrons between external leads. We predict that the resulting low-frequency current noise can be enhanced due to slow fluctuations of the shuttle oscillation energy. Moreover, at the onset of mechanical instability a pronounced peak in the low-frequency noise is expected.

Introduction. – Charge transport in nanostructures is a major research area, both theoretically and experimentally. Apart from the average current flowing through a structure in response to an applied external field, fluctuations and correlations in time of this current are of interest. By studying the current noise power spectral density (PSD), information about the charge transport process can be extracted that may not be accessible through studies of the average current alone [1]. An example of this is shot noise, arising due to the discreteness of the charge carriers (electrons) [2].

In nanoelectromechanical systems (NEMS), mechanical degrees of freedom affect and/or are affected by charge transport through the device. One such system is the single-electron shuttle system [3], also known as the nanoelectromechanical single-electron transistor (NEM-SET). The system consists of a metallic grain embedded in an elastic material between two bulk leads, forming a mechanically soft Coulomb-blockade double junction. Since current through the system is accompanied by charging of the grain, interplay between the Coulomb forces and the mechanical degrees of freedom can lead to self-oscillations of the grain, which, in turn, supports charge transport through shuttling of electrons between the leads. Much work, both experimental [4–8] and theoretical [3, 9–23], has been reported in this field. Recently there has been a lot of interest in noise in such systems [24–28].

In this paper, the noise spectrum of the single-electron shuttle is studied in the limit of weak electromechanical coupling. It is found that the onset of mechanical vibrations is accompanied by a peak in the low-frequency PSD. Hence, by measuring the noise, it can be determined whether or not the grain is oscillating. This is an important result, since direct detection of any high-frequency mechanical motion is problematic with present-day experimental techniques.

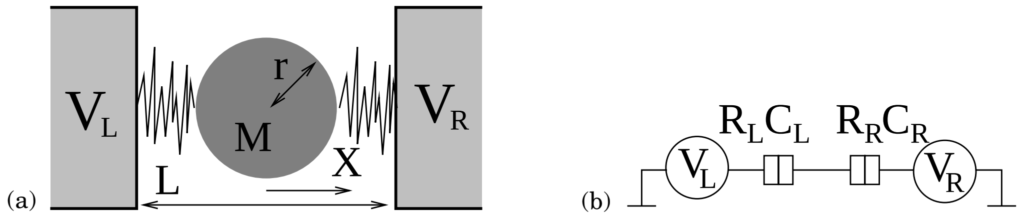

Fig. 1 – Single-electron shuttle. (a) A metallic grain of mass M and radius r placed between two leads separated by a distance L. The displacement of the grain from the center of the system is labelled X. The grain is connected to the leads via insulating elastic materials. The leads are biased to the potentials V_{L} and V_{R}. (b) Equivalent circuit of the system. The tunneling resistances and capacitances of the left and right junctions are R_{L}, R_{R}, C_{L}, and C_{R}.

Model system. – Here we give a brief introduction to the system depicted in fig. 1a. For details see ref. [12]. A metallic grain of mass M and radius r is placed between two leads via elastic, insulating materials. Applying a bias voltage $V \equiv (V_{\mathrm{L}} - V_{\mathrm{R}})$, electron transport can occur by sequential, incoherent, tunneling between the leads and the grain. This can be described using the notion of the equivalent circuit in fig. 1b which is characterized by resistances and capacitances $R_{\mathrm{L,R}}$ and $C_{\mathrm{L,R}}$ which both depend on the grain position X: $R_{\mathrm{L,R}}(X) = R_0^{\mathrm{L,R}} \exp[\pm X/\lambda]$, $C_{\mathrm{L,R}}(X) = C_0^{\mathrm{L,R}}/(1 \pm X/A_{\mathrm{L,R}})$. Here λ and $A_{\mathrm{L,R}}$ are characteristic length scales. Not shown is the grain self-capacitance C_0. If $E_C = e^2/2C \gg \hbar/R(X)C(X)$, the tunneling rates are given by the "orthodox" theory of Coulomb blockade [29]:

$$\Gamma^{\pm}_{\mathrm{L,R}}(X,V,Q) = \frac{\Delta G^{\pm}_{\mathrm{L,R}}(X,V,Q)}{e^2 R_{\mathrm{L,R}}(X)} \frac{1}{1 - e^{-\beta \Delta G^{\pm}_{\mathrm{L,R}}(X,V,Q)}}. \tag{1}$$

Here β is the inverse temperature and $\Delta G^{\pm}_{\mathrm{L,R}}(X,V,Q)$ is the decrease of free energy as the event $(Q, Q_{\mathrm{L,R}}) \to (Q \pm e, Q_{\mathrm{L,R}} \mp e)$ occurs. The charges $Q_{\mathrm{L,R}}$ and Q denote the charges accumulated on the left and right leads and the excess charge on the grain.

Considering classical, one-dimensional grain motion, we have Newton's equation $M\ddot{X} = F_{\mathrm{Ext.}}(X,V,Q)$, where $F_{\mathrm{Ext.}}$ includes an elastic force $F_k(X)$, a dissipative force $F_\gamma(\dot{X})$, an electric force $F_\epsilon(X,Q,V)$ and a vdW force $F_{\mathrm{vdW}}(X)$ yielding the equation of motion

$$M\ddot{X} = F_k(X) + F_\gamma(\dot{X}) + F_\epsilon(X,Q,V) + F_{\mathrm{vdW}}(X). \tag{2}$$

We consider the limit of low temperature and have thus neglected stochastic thermal forces. For the elastic force we use a phenomenological non-linear potential [12] acting as a harmonic well with spring force constant k for small displacements but that diverges at X_{L} and X_{R}:

$$F_k = \frac{k}{13(X_{\mathrm{L}} + X_{\mathrm{R}})} \left[\frac{(X_0 + X_{\mathrm{L}})(X_0 - X_{\mathrm{R}})^{14}}{(X - X_{\mathrm{R}})^{13}} - \frac{(X_0 - X_{\mathrm{R}})(X_0 + X_{\mathrm{L}})^{14}}{(X + X_{\mathrm{L}})^{13}} \right].$$

The dissipative force is modelled as a viscous damping term $F_\gamma = -\gamma \dot{X}$, and the electrostatic force is given by $F_\epsilon = \frac{1}{2}\frac{\mathrm{d}}{\mathrm{d}X}[Q_{\mathrm{L}}V_{\mathrm{L}} + Q_{\mathrm{R}}V_{\mathrm{R}} - QV_{\mathrm{g}}]$, where $Q_{\mathrm{L,R}}$ and the grain potential V_{g} can be calculated from the equivalent circuit of fig. 1b. The van der Waals force is

$$F_{\mathrm{vdW}} = \sum_{\zeta=\pm 1} \zeta \left[\frac{H_{\mathrm{a}} r}{6} \left(\frac{L}{2} - r - \zeta X \right)^{-2} + \frac{H_{\mathrm{r}} r}{180} \left(\frac{L}{2} - r + \zeta X \right)^{-8} \right],$$

where $H_{\mathrm{a,r}}$ are the Hamaker constants for the attractive and repulsive parts of the force. Equation (2) together with eq. (1) describe the dynamics of the system.

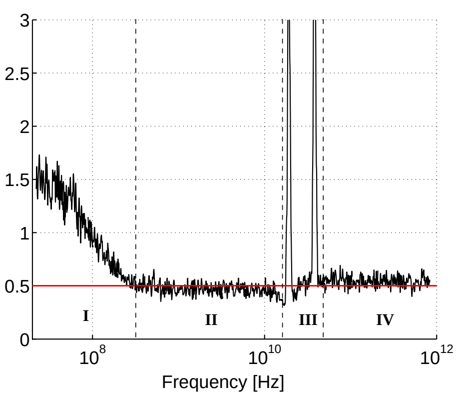

Fig. 2

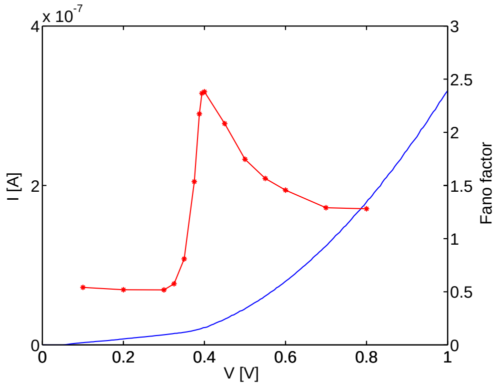

Fig. 3

Fig. 2 – Power spectrum $S_{\rm II}(\omega)$ in the shuttle regime. For frequencies above the vibrational frequency, the Fano factor is close to 1/2 as for a static Coulomb-blockade junction. The peaks are located at the frequency of vibration and at the first harmonic. For frequencies below the vibrational frequency, the in-time correlation due to the periodic grain motion leads to a slight suppression of the noise level. At still lower frequencies, the noise is increased due to slow fluctuations in mechanical energy.

Fig. 3 – Current-voltage characteristics plotted together with $S_{\rm II}(\omega \to 0)$. The current is the solid line with the scale on the left ordinate while the Fano factor is shown for a discrete set of points with the scale on the right ordinate (lines connecting the points are a guide to the eye). Below the critical voltage where there is no sustained grain motion, the Fano factor is that of a Coulomb-blockade double junction. Above the critical voltage, the grain is oscillating and the Fano factor is increased and shows a divergent behavior at the critical voltage in accordance with eq. (7).

Features of the noise spectrum. – In this section we will briefly describe the current noise spectrum of the model system presented in the previous section. Defining the current I through the system as the charge transferred per unit time from the grain to the right lead, the PSD is given by

$$S_{\rm II}(\omega) \equiv 2 \int_{-\infty}^{+\infty} \mathrm{d}t e^{i\omega t} \langle \Delta I(t) \Delta I(0) \rangle,$$

where the brackets denote ensemble averaging [30]. By doing direct numerical integration, *i.e.* solving the stochastic differential equation, eq. (2), the current as a function of time is obtained and the noise spectrum calculated. A representative result of such a calculation is shown in fig. 2. This spectrum was calculated for a system in the shuttle regime. The PSD has been normalized to obtain the Fano factor $F = S_{\rm II}/(2e\langle I \rangle)$.

We have divided the spectrum in fig. 2 into four regions marked I-IV. At high frequencies, region IV, the Fano factor is close to a value of 1/2 which is the value for a static double junction [30]. In region III two strong peaks are located at the vibration frequency and the first harmonic. This is a result of the periodic charging and decharging of the oscillating grain. The large magnitude of the first harmonic stems from the fact that charge exchange between the grain and the left lead gives rise to a displacement current in the right lead, where we measure I. Directly below the peaks, region II, the noise is suppressed below the shot noise level of a static double junction, due to the additional in time correlations between successive tunnel events induced by the oscillating grain (see also the preprints by Pistolesi [24] and by Novotny *et al.* [28]).

The most interesting part of the spectrum, however, is the low-frequency part in region I, where the Fano factor increases. This is due to low-frequency fluctuations in mechanical energy. These, in turn, lead to low-frequency fluctuations in the current resulting in enhanced low-frequency noise. One way to model the energy fluctuations is to use a stochastic differential equation with one deterministic term describing the average pumped energy and one noise term describing the fluctuations. In the next section, we present an analytical treatment of a simplified model system leading to an equation of this form (eq. (6)). Linearizing around the stable oscillation energy and using linear response for the current, one finds a contribution to the low-frequency noise given by eq. (7), explaining the low-frequency part of the spectrum.

We note that many of the features in our noise spectrum are shared by the spectrum obtained for a similar NEMS system studied by Armour [25].

Low-frequency noise for weak electromechanical coupling. – The system is completely described by the conditional probability densities $p(X,\dot{X},Q,t|X_0,\dot{X}_0,Q_0,t_0)$ to find the system with charge Q at time t in the interval $[X, X+\mathrm{d}X)$, $[\dot{X},\dot{X}+\mathrm{d}\dot{X})$ given it was located around $(X_0,\dot{X}_0,Q_0)$ at time t_0. The time evolution of the conditional probability density, as well as of the unconditional probability density $p(X,\dot{X},Q,t)$, is given by the phase space equation

$$\begin{aligned}\frac{\partial}{\partial t}p\big(X,\dot{X},Q,t\big) &= -\frac{\partial}{\partial X}\big(\dot{X}p\big(X,\dot{X},Q,t\big)\big)+\frac{\partial}{\partial \dot{X}}\left(\frac{\gamma\dot{X}-kX+F(Q)}{M}p\big(X,\dot{X},Q,t\big)\right)+\\ &+\sum_{Q'\neq Q}\Gamma_{Q'\to Q}(X)p\big(X,\dot{X},Q',t\big)-\sum_{Q'\neq Q}\Gamma_{Q\to Q'}(X)p\big(X,\dot{X},Q,t\big). \qquad (3)\end{aligned}$$

Here a simplified version of the external force $F_{\text{Ext.}}=\gamma\dot{X}-kX+F(Q)$, where $F(Q)\equiv F_\epsilon(X=0,Q,V)$, has been used. Introducing action-angle variables (E,ϕ) defined through $(X,\dot{X})=\sqrt{2E/M\omega^2}(\sin(\phi),\omega\cos(\phi))$, where $\omega^2\equiv k/M$, eq. (3) takes the form

$$\begin{aligned}\frac{\partial}{\partial t}p(E,\phi,Q,t) &= -\frac{\partial}{\partial\phi}\left(\left[\omega+\frac{\gamma}{M}\sin\phi\cos\phi-\frac{F(Q)\sin\phi}{\sqrt{2ME}}\right]p(E,\phi,Q,t)\right)-\\ &-\frac{\partial}{\partial E}\left(\left[-2\frac{\gamma}{M}E\cos^2\phi+\sqrt{\frac{2E}{M}}F(Q)\cos(\phi)\right]p(E,\phi,Q,t)\right)+\\ &+\sum_{Q'\neq Q}\Gamma_{Q'\to Q}(E,\phi)p(E,\phi,Q',t)-\sum_{Q'\neq Q}\Gamma_{Q\to Q'}(E,\phi)p(E,\phi,Q,t). \qquad (4)\end{aligned}$$

To facilitate an analytical treatment, it is convenient to rewrite eq. (4). We thus introduce the dimensionless quantities $\tau=t\omega$, $n=Q/e$, $f_n=F(ne)/F(e)$, $\mathcal{E}=E/(\frac{1}{2}M\omega^2\lambda^2)$, $\tilde{\Gamma}_{n\to n'}=\omega^{-1}\Gamma_{n\to n'}$, $\delta=F(e)/k\lambda$, and $\eta=\gamma/(M\omega)$. Both δ and η are small parameters and we can define $\epsilon=\sqrt{\delta\eta}$ and $\iota=\sqrt{\delta/\eta}$ which are suitable for perturbation theory. The probability density can be written in vectorial form as $\boldsymbol{P}(\mathcal{E},\phi,\tau)$, where the i-th component is given by $p(\mathcal{E},\phi,n(i),\tau)$ with $n(i)\equiv(-1)^{i-1}\mathrm{Int}[\frac{i}{2}]$. We also introduce the matrices

$$\hat{I}_{i,j}=\delta_{i,j},\qquad \hat{f}_{i,j}\equiv\delta_{i,j}f_{n(i)},\qquad \hat{\Gamma}^{+}_{i,j}=\tilde{\Gamma}_{n(j)\to n(i)},\qquad \hat{\Gamma}^{-}_{i,j}=\delta_{i,j}\sum_{n'}\tilde{\Gamma}_{n(i)\to n'},$$

and define three operators $\hat{\mathcal{L}}_1=-\frac{\partial}{\partial\phi}+\hat{\Gamma}^{+}(\mathcal{E},\phi)-\hat{\Gamma}^{-}(\mathcal{E},\phi)$, $\hat{\mathcal{L}}_2=\frac{\partial}{\partial\phi}[\iota\frac{\hat{f}}{\sqrt{\mathcal{E}}}\sin\phi-\iota^{-1}\hat{I}\sin\phi\cos\phi]$, and $\hat{\mathcal{L}}_3=2\frac{\partial}{\partial\mathcal{E}}[\hat{I}\iota^{-1}\mathcal{E}\cos^2\phi-\iota\hat{f}\sqrt{\mathcal{E}}\cos\phi]$. Equation (4) can then be compactly written as

$$\frac{\partial}{\partial\tau}\boldsymbol{P}(\mathcal{E},\phi,\tau)=\big[\hat{\mathcal{L}}_1+\epsilon\big(\hat{\mathcal{L}}_2+\hat{\mathcal{L}}_3\big)\big]\boldsymbol{P}(\mathcal{E},\phi,\tau).$$

Since the low-frequency noise is governed by a time scale much longer than the period of vibration, adiabatic elimination of fast variables can be used to treat slow fluctuations in energy. This amounts to doing perturbation theory in ϵ.

Following ref. [31], we let $\boldsymbol{P}_\lambda$ and $\boldsymbol{Q}_\lambda$ be normalized eigensolutions to $\hat{\mathcal{L}}_1\boldsymbol{P}_\lambda = \lambda(\mathcal{E})\boldsymbol{P}_\lambda$ and $\hat{\mathcal{L}}_1^\dagger\boldsymbol{Q}_\lambda = \lambda^*(\mathcal{E})\boldsymbol{Q}_\lambda$, corresponding to eigenvalue λ. $\boldsymbol{P}_0(\mathcal{E},\phi)$ is the stationary solution to the unperturbed problem, *i.e.*, $\hat{\mathcal{L}}_1\boldsymbol{P}_0 = 0$, while $\boldsymbol{Q}_0$ solves the adjoint equation $\hat{\mathcal{L}}_1^\dagger\boldsymbol{Q}_0 = 0$. The projector $\hat{\mathcal{P}}_0$ onto this state acting on an arbitrary vector $\boldsymbol{x}(\mathcal{E},\phi,\tau)$ is given by

$$\big(\hat{\mathcal{P}}_0\boldsymbol{x}\big)(\mathcal{E},\phi,\tau) = \boldsymbol{P}_0(\mathcal{E},\phi)\int_0^{2\pi}\mathrm{d}\phi'\boldsymbol{Q}_0^*(\mathcal{E},\phi')\cdot\boldsymbol{x}(\mathcal{E},\phi',\tau).$$

By direct insertion, using that $\hat{\mathcal{L}}_1^\dagger = \frac{\partial}{\partial\phi} + \hat{\mathcal{G}}^\top(\mathcal{E},\phi)$, one finds that $(\boldsymbol{Q}_0)_n = [1,1,\dots,1]^\top$. Next, splitting up $\boldsymbol{P}(\mathcal{E},\phi,\tau)$ in mutually orthogonal parts $\boldsymbol{v}\equiv\hat{\mathcal{P}}_0\boldsymbol{P}$ and $\boldsymbol{w}\equiv(1-\hat{\mathcal{P}}_0)\boldsymbol{P}$, an equation, correct to second order in ϵ, can be found for $\boldsymbol{v}$:

$$\frac{\partial}{\partial\tau}\boldsymbol{v} = \epsilon\hat{\mathcal{P}}_0\hat{\mathcal{L}}_4\boldsymbol{v} - \epsilon^2\hat{\mathcal{P}}_0\hat{\mathcal{L}}_3\hat{\mathcal{L}}_1^{-1}\big[\hat{\mathcal{L}}_2+\hat{\mathcal{L}}_3-\hat{\mathcal{P}}_0\hat{\mathcal{L}}_4\big]\boldsymbol{v}. \tag{5}$$

Here $\epsilon\hat{\mathcal{L}}_4 = \hat{I}\frac{\partial}{\partial\mathcal{E}}[\gamma(\mathcal{E})-\mathcal{W}(\mathcal{E})]$, which contains the average dissipation per cycle $\gamma(\mathcal{E})$ and the average pumped energy per cycle $\mathcal{W}(\mathcal{E})$ defined through

$$\gamma(\mathcal{E})\equiv 2\eta\mathcal{E}\int_0^{2\pi}\mathrm{d}\phi\boldsymbol{Q}_0^*\cdot\boldsymbol{P}_0(\mathcal{E},\phi)\cos^2\phi,\qquad \mathcal{W}(\mathcal{E}) = 2\delta\sqrt{\mathcal{E}}\int_0^{2\pi}\mathrm{d}\phi\boldsymbol{Q}_0^*\cdot\hat{f}\boldsymbol{P}_0(\mathcal{E},\phi)\cos\phi.$$

Letting $\rho(\mathcal{E},\tau)$ be the probability density for finding the system with mechanical energy $\mathcal{E}$, *i.e.* $\boldsymbol{v}=\boldsymbol{P}_0\rho$, and using eq. (5), a Fokker-Planck equation for ρ is obtained:

$$\frac{\partial}{\partial\tau}\rho(\mathcal{E},\tau) = -\frac{\partial}{\partial\mathcal{E}}\big[\big(\mathcal{W}(\mathcal{E})-\gamma(\mathcal{E})+\mathcal{O}(\epsilon^2)\big)\rho(\mathcal{E},\tau)\big] - \epsilon^2\frac{\partial^2}{\partial\mathcal{E}^2}\left(\sum_{\lambda\neq 0}\frac{f_\lambda(\mathcal{E})g_\lambda(\mathcal{E})}{\lambda(\mathcal{E})}\rho(\mathcal{E},\tau)\right),$$

where $f_\lambda(\mathcal{E})\equiv\int_0^{2\pi}\mathrm{d}\phi\boldsymbol{Q}_0^*\cdot\hat{\mathcal{O}}\boldsymbol{P}_\lambda(\mathcal{E},\phi)$ and $g_\lambda(\mathcal{E})\equiv\int_0^{2\pi}\mathrm{d}\phi\boldsymbol{Q}_\lambda^*\cdot\hat{\mathcal{O}}\boldsymbol{P}_0(\mathcal{E},\phi)$, with $\hat{\mathcal{O}}\equiv[2\iota^{-1}\mathcal{E}\cos^2\phi - 2\iota\hat{f}\sqrt{\mathcal{E}}\cos\phi]$. Since $(\mathcal{W}(\mathcal{E})-\gamma(\mathcal{E}))$ is of order ϵ, the small energy shift of order ϵ^2 can be ignored to a first approximation and an equivalent Ito stochastic differential equation for the vibrational energy $\mathcal{E}$ is arrived at:

$$\mathrm{d}\mathcal{E} = \big[\mathcal{W}(\mathcal{E})-\gamma(\mathcal{E})\big]\mathrm{d}\tau + \alpha(\mathcal{E})\mathrm{d}W(\tau), \tag{6}$$

where $W(\tau)$ is the Wiener process and $\alpha(\mathcal{E})\equiv\epsilon\sqrt{-2\sum_{\lambda\neq 0}f_\lambda(\mathcal{E})g_\lambda(E)}$.

Performing a small noise expansion [31], *i.e.* linearizing eq. (6) around $\mathcal{E}_0$, where $\mathcal{E}_0$ solves $(\mathcal{W}(\mathcal{E}_0)-\gamma(\mathcal{E}_0))=0$, one finds

$$\mathrm{d}(\delta\mathcal{E}) = \big[W'(\mathcal{E}_0)-\gamma'(\mathcal{E}_0)\big]\delta\mathcal{E}\,\mathrm{d}\tau + \alpha(\mathcal{E}_0)\mathrm{d}W(\tau).$$

The correlation function for $\delta\mathcal{E}$ is then

$$\langle\delta\mathcal{E}(\tau)\delta\mathcal{E}(0)\rangle = \frac{\alpha(\mathcal{E}_0)^2}{2}\frac{e^{-[\gamma'(\mathcal{E}_0)-W'(\mathcal{E}_0)]|\tau|}}{\gamma'(\mathcal{E}_0)-W'(\mathcal{E}_0)}\,.$$

Using linear response to evaluate the current, *i.e.* $I(\mathcal{E}) = I(\mathcal{E}_0)+I'(\mathcal{E}_0)\delta\mathcal{E}$, an analytical expression for the contribution to the PSD from low-frequency fluctuations in the mechanical energy can be obtained:

$$S_{\mathrm{II}}(\omega) = 2\frac{[\alpha(\mathcal{E}_0)I'(\mathcal{E}_0)]^2}{(\gamma'(\mathcal{E}_0)-\mathcal{W}'(\mathcal{E}_0))^2+\omega^2}\,. \tag{7}$$

TABLE I – *Numerical values of parameters used to obtain data of fig.* 3.

Quantity	Value	Units	Quantity	Value	Units	Quantity	Value	Units
L	5	nm	k	1	N/m	λ	0.1	nm
r	1	nm	X_{L}, X_{R}	1	nm	R_0^{L}, R_0^{R}	10	MΩ
M	10^{-23}	kg	H_{a}	$4\cdot10^{-19}$	Nm	C_0^{L}, C_0^{R}, C_0	1	aF
γ	10^{-13}	kg/s	H_{r}	10^{-72}	Nm^7	A_{L}, A_{R}	2.5	nm

Here the current I is given by $I(\mathcal{E}) = \frac{e\omega}{2\pi}\int_0^{2\pi} \mathrm{d}\phi \boldsymbol{Q}_0^* \cdot \hat{\mathcal{J}}(\mathcal{E},\phi)\boldsymbol{P}_0(\mathcal{E},\phi)$, where $(\hat{\mathcal{J}}(\mathcal{E},\phi))_{i,j} \equiv \delta_{i,j}\tilde{\Gamma}^{\mathrm{R}}_{n(i)\to n(i)-1}(\mathcal{E},\phi) - \tilde{\Gamma}^{\mathrm{R}}_{n(i)\to n(i)+1}(\mathcal{E},\phi)$ is the current operator.

Equation (7) is our central result. Two important conclusions can be drawn from this equation. First, for $I'(\mathcal{E}_0) \neq 0$, below a break frequency given by $\omega_{\mathrm{c}} = (\gamma'(\mathcal{E}_0) - \mathcal{W}'(\mathcal{E}_0))$ the noise will rise due to fluctuations in oscillation energy. This agrees with the PSD in fig. 2. Second, a stable non-zero oscillation energy $\mathcal{E}_0$ necessarily requires $\gamma'(\mathcal{E}_0) - \mathcal{W}'(\mathcal{E}_0) > 0$ (see ref. [9]). The transition from shuttle to stationary regime occurs when $\gamma'(\mathcal{E}_0) = \mathcal{W}'(\mathcal{E}_0)$ which implies that the low-frequency noise may display a divergent behavior at the point of transition. This is in agreement with a recent semiclassical treatment by Novotny *et al.* [28].

To investigate this, eqs. (1)-(2) were simulated for a sequence of voltages for one typical system and the resulting *I*-*V* curve as well as the Fano factor are shown in fig. 3. The parameter values used are shown in table I. They correspond to a nanometer-sized Au grain commonly used in experiments with self-assembled Coulomb-blockade double junctions. Although, as explained in [12], the non-parabolic confining potential smears any step-structure in the current-voltage characteristics, the transition between static- and shuttle-operation is clearly visible in the noise spectrum. In accordance with eq. (7), on approaching the threshold from above (higher to lower voltages) the PSD shows divergent behavior. Below the threshold voltage the Fano factor is of the order 1/2.

In the shuttle regime, well above the threshold voltage, the Fano factor is increased. Should the potential be such that $I'(\mathcal{E}_0) \to 0$ for large $\mathcal{E}_0$ (as, for instance, for a harmonic potential), the LF noise would not be enhanced. In terms of fig. 2, this would mean that the lowered noise level in region II is continued into region I. Note that, even though eqs. (6)-(7) were derived for a harmonic potential, this derivation can be generalized to the non-linear case since any oscillatory motion can be described in an energy-phase space $(\mathcal{E},\phi)$ although with other periodic functions than $\sin\phi$ and $\cos\phi$.

Conclusions. – Using adiabatic elimination of fast variables and numerical integration of eqs. (1)-(2), the PSD of the classical single-electron shuttle has been studied in the case of weak electromechanical coupling. We have focussed on the low-frequency part of the spectrum, which is the part most susceptible to direct measurements, and found that the shuttle regime can be distinguished from the stationary regime by the noise level at low frequencies.

In particular, the shuttle regime is associated with a rise in the low-frequency PSD, as compared to a stationary Coulomb-blockade double junction, resulting in an increased Fano factor. This increase is due to slow variations in the current arising from variations in oscillation energy. Approaching the point of the transition from above (lowering the bias voltage when in the shuttle regime), the noise level shows a (quasi) divergent behavior. Hence, even though a measurement of the average current alone may not reveal whether the system is in the shuttle regime or not, the accompanying noise signature can provide this piece of information.

* * *

The authors are grateful for stimulating discussions with R. I. Shekhter and L. Y. Gorelik. This work has received financial support (AI) through The Swedish Foundation for International Cooperation in Research and Higher Education (STINT), and (TN) the Swedish Research Council (VR).

REFERENCES

[1] Blanter Ya. M. and Buttiker M., *Phys. Rep.*, **336** (2000) 1.
[2] Hanke U., Galperin Y. M., Chao K. A. and Zou N., *Phys. Rev. B*, **48** (1993) 48.
[3] Gorelik L. Y. *et al.*, *Phys. Rev. Lett.*, **80** (1998) 4526.
[4] Erbe A. *et al.*, *Appl. Phys. Lett.*, **73** (1998) 3751; Erbe A., Weiss C., Zwerger W. and Blick R. H., *Phys. Rev. Lett.*, **87** (2001) 096106.
[5] Scheible D. V., Erbe A. and Blick R. H., *New J. Phys.*, **4** (2002) 86.
[6] Park H. *et al.*, *Nature (London)*, **407** (2000) 57.
[7] Nagano K., Okuda A. and Majima Y., *Appl. Phys. Lett.*, **81** (2002) 544.
[8] Tuominen M. T., Krotkov R. V. and Breuer M. L., *Phys. Rev. Lett.*, **83** (1999) 3025.
[9] Isacsson A. *et al.*, *Physica B*, **255** (1998) 150.
[10] Nishiguchi N., *Phys. Rev. B*, **65** (2001) 035403.
[11] Nord T. *et al.*, *Phys. Rev. B*, **65** (2002) 165312.
[12] Nord T. and Isacsson A., *Phys. Rev. B*, **69** (2004) 035309.
[13] Weiss C. and Zwerger W., *Europhys. Lett.*, **47** (1999) 97.
[14] Nishiguchi N., *Phys. Rev. Lett.*, **89** (2002) 66802.
[15] Boese D. and Schoeller H., *Europhys. Lett.*, **54** (2001) 668.
[16] Fedorets D. *et al.*, *Europhys. Lett.*, **58** (2002) 99.
[17] Armour A. D. and MacKinnon A., *Phys. Rev. B*, **66** (2002) 035333.
[18] Fedorets D., *Phys. Rev. B*, **68** (2003) 033106.
[19] Novotný T., Donarini A. and Jauho A.-P., *Phys. Rev. Lett.*, **90** (2003) 256801.
[20] McCarthy K. D., Prokof'ev N. and Tuominen M. T., *Phys. Rev. B*, **67** (2003) 245415.
[21] Braig S. and Flensberg K., *Phys. Rev. B*, **68** (2003) 205324.
[22] Gorelik L. Y. *et al.*, *Nature (London)*, **411** (2001) 454; Isacsson A. *et al.*, *Phys. Rev. Lett.*, **89** (2002) 277002.
[23] Shekhter R. I. *et al.*, *J. Phys. Condens. Matter*, **15** (2003) 441.
[24] Pistolesi F., cond-mat/0401361.
[25] Armour A., cond-mat/0401387.
[26] Chtchelkatchev N. M., Belzig W. and Bruder C., cond-mat/0401486.
[27] Romito A. and Nazarov Yu. V., condmat/0402412.
[28] Novotny T. *et al.*, cond-mat/0402597.
[29] Kulik I. O. and Shekhter R. I., *Sov. Phys. JETP*, **41** (1975) 308.
[30] de Jong M. J. M. and Beenakker C. W. J., in *Mesoscopic Electron Transport*, edited by Sohn L. L. *et al.* (Kluwer, The Netherlands) 1997.
[31] Gardiner C. W., *Handbook of Stochastic Methods*, 2nd edition (Springer, Berlin) 1997.